Fish and Shellfish Immunology 84 (2019) 599–608

Contents lists available at ScienceDirect

Fish and Shellfish Immunology

journal homepage: www.elsevier.com/locate/fsi

Full length article

Characterization, expression profiling and functional characterization of cathepsin Z (CTSZ) in turbot (*Scophthalmus maximus* L.)

Xin Cai, Chengbin Gao, Huanhuan Song, Ning Yang, Qiang Fu, Fenghua Tan, Chao Li*

Marine Science and Engineering College, Qingdao Agricultural University, Qingdao, 266109, China

ARTICLE INFO

Keywords:
CTSZ
Turbot
Vibrio anguillarum
Streptococcus iniae
Mucosal immunity

ABSTRACT

Cathepsin Z (CTSZ) is a lysosomal cysteine protease of the papain superfamily. It participates in the host immune defense via phagocytosis, signal transduction, cell-cell communication, proliferation, and migration of immune cells such as monocytes, macrophages, and dendritic cells. In this study, we reported the identification of *Sm*CTSZ, a CTSZ homolog from turbot (*Scophthalmus maximus* L.). *Sm*CTSZ was 317 residues in length and contains a Pept-C1 domain. In multiple species comparison, *Sm*CTSZ shared 65–93% overall sequence identities with the CTSZ counterparts from human, rat, and several fish species. In the phylogenetic analysis, *Sm*CTSZ showed the closest relationship to *Cynoglossus semilaevis*. The syntenic analysis revealed the similar neighboring genes of CTSZ across all the selected species, which suggested the synteny encompassing CTSZ region during vertebrate evolution. Subsequently, *Sm*CTSZ was constitutively expressed in various tissues, with the lowest and highest levels in brain and intestine respectively. In addition, *Sm*CTSZ was significantly up-regulated in intestine following both Gram-negative bacteria *Vibrio anguillarum*, and Gram-positive bacteria *Streptococcus iniae* immersion challenge. Finally, the *rSm*CTSZ showed strong binding ability to all the examined microbial ligands, and the agglutination effect to different bacteria. Taken together, these results indicated *Sm*CTSZ could play important roles in mucosal immune response in the event of bacterial infection in teleost. However, the knowledge of CTSZ are still limited in teleost species, further studies should be carried out to better characterize its detailed roles in teleost mucosal immunity.

1. Introduction

Cathepsin Z (CTSZ), one of the 11 cysteine proteases members of papain family, represents the major component of lysosomal proteolysis system [1]. According to the structural similarities, it is also denoted as cathepsin X (CTSX) [2], P (CTSP) [3] or Y(CTSY) [4]. CTSZ shows several unique features in enzyme activity properties and gene structure. In particular, the proregion of cathepsin Z is quite short compared to other cathepsins [5]. The mature form of cathepsin Z has an ECD motif (Glu-Cys-Asp) playing important roles in integrin-mediated signal transduction [6]. Moreover, cathepsin Z exhibits carboxy-monopeptidase as well as carboxy-dipeptidase activities at its C terminus [7]. In comparison to other cathepsins, cathepsin Z is the most similar to cathepsin B, but the C terminus of the mature cathepsin Z functionally shows only monopeptidase activity, and not acting as an endopeptidase in contrast to cathepsin B [8]. In human, cathepsin Z plays important housekeeping roles as a lysosomal digestive enzyme similar to cathepsin B, L, H, and O [9].

Cathepsins are involved in antigen processing and maturation of the major histocompatibility complex class II molecules in the immune system. Thereinto, CTSZ is mostly expressed in immune cells, such as macrophages and monocytes [9–11]. Although CTSZ is the most recent addition to cathepsins family, most of its biological functions related to cathepsin have been established in mammals. Recently, a number of CTSZ genes have been discovered and characterized at the molecular level from several fish species. For example, in carp (*Cyprinus carpio*), CTSZ was widely expressed in carp tissues and showed critical roles in yolk metabolism [12]. Additionally, CTSZ was known to be involved in vitellogenesis and oocyte maturation of the mummichog (*Fundulus heteroclitus*) [13], proteolytic activity on vitellogenin in carp [14], and food digestion in starfish (*Asterina pectinifera*) [15]. But its detailed immune roles against pathogen infection are still limited in a handful teleost species, for instance, CTSZ has been observed to play bactericidal role in epidermal mucus in carp [14].

Turbot (*Scophthalmus maximus* L.), one of representative species of flatfish, is mainly distributed in the northeast of Atlantic, and was introduced into China in 1992. Following rapid development, it has become one of the most extensively maricultured species in China.

* Corresponding author.
E-mail address: leoochao@163.com (C. Li).

https://doi.org/10.1016/j.fsi.2018.10.046
Received 22 July 2018; Received in revised form 10 October 2018; Accepted 20 October 2018
Available online 22 October 2018
1050-4648/

However, bacterial disease have resulted in dramatic economic losses to turbot farming industry. In order to develop disease control and prevention measures, many efforts have been made to identify the immune genes, as well as their associate immune activities following infection in turbot [16–20]. In addition, the mucosal immune system is the first line of host defense against pathogen infection, a better understanding of mucosal immunity against infection is urgent for aquaculture research to improve immunity of fish via immersion or feeding [21]. In this regard, we identified and characterized CTSZ gene in turbot, and its expression patterns in mucosal tissues (skin, gill and intestine) following different bacterial infection, as well as the binding ability to microbial ligands.

2. Materials and methods

2.1. Bacteria challenge and sample collection

Turbot were obtained from commercial fish farm in Haiyang (Shandong Province, China) and maintained in the Aquatic Facility of Marine Science and Engineering College, Qingdao Agricultural University. The fish were kept at 18 °C using a flow-through water system and a simulated natural photoperiod. Fish were fed to satiation daily with commercial pellets, and acclimated for at least 2 weeks prior to conduct experiments.

In order to investigate the immune roles of CTSZ gene in the host defense against bacterial infection, the Gram-negative bacteria *V. anguillarum* and the Gram-positive bacteria *S. iniae* were selected to conduct the bath challenge. After a pre-challenge, the bacteria were re-isolated from symptomatic fish and biochemically confirmed to be infected with *V. anguillarum* and *S. iniae*, respectively. The concentration of the bacteria was determined using colony forming unit (CFU) per mL by plating 1 mL of 10-fold serial dilutions onto LA agar plates. At each timepoint following challenge, skin, gill and intestine samples were collected from 15 fish (5 fish per pool) from the appropriate aquaria after anaesthetizing.

Briefly, the *S. iniae* isolate was inoculated in LB medium in a shaker incubator at 28 °C overnight. The fish were equally divided into five aquariums, 4 challenged groups (2 h, 4 h, 8 h and 12 h) and one control group. For the challenge, the fish were immersed for 2 h at a final concentration of 5×10^6 CFU/mL, while the control fish were immersed in sterilized media alone.

The *V. anguillarum* was inoculated in LB broth in a shaker (180 rpm) at 28 °C overnight. The fish were immersed at a final concentration of 5×10^7 CFU/mL for 2 h, while the control fish were immersed in sterilized media alone. Aquaria were randomly assigned for 2 h, 6 h, 12 h and 24 h post-treatment and 0 h control with 30 fish in each aquarium for sample collection. All samples from both experiments were flash-frozen in liquid nitrogen and then stored in a - 80 °C ultra-low freezer until preparation of RNA.

2.2. Sequence identification and analysis

The turbot CTSZ gene was captured in transcriptome and genome databases by TBLASTN program using CTSZ protein sequences from other species as queries with a cutoff E-value of $1e^{-10}$ [22,23]. The retrieved initial pool of sequences were aligned to delete the repeated entries to generate a set of unique sequences for further analysis. Upon identification, the candidate sequences were then translated using ORF Finder (https://www.ncbi.nlm.nih.gov/orffinder/). The predicted ORF sequences were further verified by BLASTP (http://blast.ncbi.nlm.nih.gov/Blast.cgi) against NCBI non-redundant protein sequence database. The conserved domains and signal peptides were further identified by the simple modular architecture research tool (SMART; http://smart.embl-heidelberg.de/). The molecular mass, theoretical pI, and *N*-glycosylation sites were analyzed by ExPASy server [24]. The percentages of similarity and identity were calculated by MatGAT program [25]. The secondary structure of the CTSZ could be browsed on the Pole Bioinformatique Lyonnais (PBIL) server (https://prabi.ibcp.fr/htm/index.php). The presumed 3D protein structural model was established using protein homology/analogy recognition engine V 2.0 (Phyre2) (http://www.sbg.bio.ic.ac.uk/phyre2/html/page.cgi?id=index). Finally, the identified sequence was validated by the regular sanger sequencing.

2.3. Sequence alignment, phylogenetic and syntenic analysis

The phylogenetic tree was constructed based on the amino acid sequences of CTSZ from various species retrieved from GenBank, including human (*Homo sapiens*), mouse (*Mus musculus*), chicken (*Gallus gallus*), painted turtle (*Chrysemys picta*), western clawed frog (*Xenopus tropicalis*), zebrafish (*Danio rerio*), large yellow croaker (*Larimichthys crocea*), half smooth togue sole (*Cynoglossus semilaevis*), Channel catfish (*Ictalurus punctatus*), northern pike (*Esox lucius*), guppy (*Poecilia reticulata*), mummichog (*Fundulus heteroclitus*) and turbot (*S. maximus*). Clustal Omega program was utilized to perform the multiple protein sequence alignment [26]. A neighbor-joining phylogenetic tree was generated using the Molecular Evolutionary Genetics Analysis (MEGA 7) software [27]. Data were analyzed using Poisson distance correction and gaps were removed by complete deletion. To evaluate the topological stability of the phylogenetic tree, bootstrapping with 1000 replications was conducted.

In order to further verify the characterization of turbot CTSZ gene, syntenic analysis was performed with human, mouse, chicken and fugu. Briefly, using FGENESH program, the protein sequences of neighboring genes of the turbot CTSZ was predicted from the turbot scaffold. The identified protein sequences were annotated against NCBI non-redundant (nr) database by BLASTP. Ensembl database and Genomicus were used to determine the conserved syntenic pattern of CTSZ gene in other species [28].

2.4. Real-time PCR analysis of CTSZ expression following bacterial challenge

Total RNA was isolated using Trizol® Reagent (Invitrogen, USA) according to manufacturer's instruction. Total RNA were extracted and treated with RNase-free DNaseIto remove genomic DNA contamination. The quality and quantity of each RNA sample were measured on a Nanodrop 2000 (Thermo Electron North America LLC, FL). A260/280 ratio of all extracted samples were greater than 1.8. One microgram of total RNA was used for cDNA synthesis with PrimeScript RT reagent Kit with gDNA Eraser (Takara, Dalian, China) according to the manufacturer's instruction. QPCR was carried out in CFX96 Touch (Bio-Rad Laboratories, CA, USA) using the SYBR ExScript qRT-PCR Kit (Takara, Dalian, China) following the manufacturer's instructions. The PCR reaction mixture was denatured at 95 °C for 30 s and then subjected to 40 cycles of 95 °C for 5 s, 58 °C for 5 s and followed by dissociation curve analysis, 5 s at 65 °C, then up to 95 °C at a rate of 0.1 °C/s increment, to verify the specificity of the amplicons. Triple RNA samples at each timepoint were analyzed for gene expression. And turbot 18S rRNA gene was used as an internal control for normalization of the expression levels (gene specific primer was designed using primer3 software and shown in Table 1). The fold differences were calculated by the relative quantification method using the Relative Expression Software Tool (REST) to capture significance at the level of $P < 0.05$ [29].

2.5. Plasmid construction

In order to construct the expression plasmid for turbot CTSZ, the open reading frame without signal sequence of CTSZ was amplified with the specific primers following cDNA synthetization (Table 1). After gel extraction, the PCR products were ligated to pEASY-Blunt-E1 vector, and then transformed into competent Trans1-T1 cells. Following blue-

Table 1
Primers used in this study.

Primer Name	Sequences (5′-3′)	Information
*Sm*CTSZ-P-F	GCAGGAGCGTCGTTCCG	Primer used to obtain ORF
*Sm*CTSZ-P-R	CTAGAGGTCGTCCTTCGGG	without signal peptide
T7 test	TAATACGACTCACTATA	Specific primer for pEASY-Blunt-
T7 Primer	CCACCGCTGAGCAATAACTA	E1 vector
18S-F	ATGGCCGTTCTTAGTTGGTG	Q-PCR primer for control
18S-R	CTCAATCTCGTGTGGCTGAA	
*Sm*CTSZ-F	ATTCAACGTCGTCCTCCACT	Q-PCR primer
*Sm*CTSZ-R	CGGAGTGTGCAACATTGTGA	

white spotting selection, the positive clones were selected and sequenced with T7 Promoter Primer. The verified recombinant plasmid was extracted and marked as pEASY-E1-CTSZ. Sequence analysis revealed that one of the plasmids contains the open reading frame without signal sequence of a CTSZ homolog (named *Sm*CTSZ for "*S. maximus* CTSZ").

2.6. Production and purification of recombinant protein (rSmCTSZ)

To obtain recombinant *Sm*CTSZ protein, the recombinant plasmid pEASY-E1-CTSZ was transformed into *E. coli* BL21 (DE3). The transformant BL21- CTSZ and the control BL21 with empty pET-32a were cultured in LB-kanamycin at 37 °C with shaking at 200 rpm. When the culture medium reached an OD600 of 0.4–0.6, IPTG was added to the medium at a final concentration of 0.9 mM and incubated for another 4 h optimal time. Recombinant protein was purified using by nickel-nitrilotriacetic acid chromatography (Takara, China) according to the instructions of the manufactures, and analyzed by 12% sodium dodecylsulfate polyacrylamide gel electrophoresis (SDS-PAGE) and visualized by staining with Coomassie brilliant blue. The concentration of the recombinant protein was determined using Bradford's method.

2.7. Western blot

Sodium dodecyl sulfate polyacrylamide gel electrophoresis (SDS-PAGE) was carried out on a 7.5 cm by 8.5 cm polyacrylamide gel of 1 mm thickness in a vertical gel electrophoresis apparatus to detect the antigenic determinants of molecular weight. *rSm*CTSZ preparations were mixed with 5 μl of tracking dye and heated in a water bath for 5 min; then were electrophoresed on a 5% stacking gel and a 12% separating gel. The gel was initially run at 60 V until the tracking dye reached the separating gel and then the voltage was increased to 80 V until the dye reached the bottom of the gel. One gel was stained with 0.25% Coomassie Brilliant Blue R-250, destained and analyzed. Another gel was transferred to a polyvinylidene fluoride (PVDF) at 300 mA constant current for 1 h and washed three times for 5 min with PBS. The PVDF was blocked with 3% bovine albumin for 1 h at 37 °C and washed three times for 5 min each with PBST. The PVDF was then incubated in Anti-His Tag Mouse Monoclonal Antibody (Solarbio, Beijing, China) for 1 h at 37 °C followed by three washings with PBST. After this, the PVDF was incubated in goat anti-mouse IgG/HRP (Solarbio, Beijing, China) for 1 h at 37 °C and washed as above. The PVDF reacted in a solution of TMB Single-Component Substrate (Solarbo) for 15 min then the reaction was terminated and observations were made.

2.8. Solid-phase enzyme-linked immunosorbent assay (ELISA)

The binding ability of *rSm*CTSZ with lipopolysaccharide (LPS), lipoteichoic acid (LTA) and peptidoglycan (PGN) was detected by the method of ELISA. Briefly, LPS/LTA/PGN (5 μg/mL) were coated to a 96-well plate at 4 °C overnight. The plates were rinsed with PBS-Tween (PBS containing 0.05% (w/v) Tween 20) three times and blocked for 1 h with PBS-Tween 5% BSA at 37 °C. After three washes with PBS-Tween, 100 μl of the control protein with empty pET-32a or the increasing concentrations of purified recombinant *Sm*CTSZ (5, 10, 20, 40, and 80 μg/mL) were added into each ligand-coated well, with four replicates for each concentration, and incubated at 37 °C for 1 h, and the plates were rinsed three times with PBS-Tween. Then, the wells were incubated at 37 °C for 1 h with 100 μl mouse anti-His antibody (Solarbio, Beijing, China) (diluted 1:1000 in 5% BSA), after three washes followed by another incubation at 37 °C for 40 min, another three washings with PBS-Tween, 100 μl horseradish peroxidase conjugated goat anti-mouse IgG (Solarbio, Beijing, China) (diluted 1:1000 in 5% BSA) were added to each well. After 30 min of incubation in darkness, the reaction was terminated by adding 0.5 M sulfate, and the plate was then read at $OD_{450\ nm}$ with an ELISA plate reader (EL800, BioTek, with the Gen 5 program).

2.9. Agglutination of FITC-labeled recombinant SmCTSZ to four species of bacteria

S. agalactiae, *V. anguillarum*, *E. coli* and *S. iniae* were cultured in Luria-Bertani broth in a shaker incubator (180 rpm) at 28 °C overnight. The bacteria were harvested by centrifugation at 5000 g for 10 min and resuspended with TBS-Ca (20 mM Tris-HCL, 150 mM NaCl, 20 mM $CaCl_2$, PH = 8.0) for twice and adjusted to 2.5×10^9 CFU/mL. Purified protein r*Sm*CTSZ was dialyzed in PBS for 12 h in 4 °C for twice and adjusted concentration to 2 mg/mL. Then r*Sm*CTSZ was dyed by HOOK™ Dye Labeling Kit (G-Biosciences, USA) according to manufacturer's instructions. Briefly, the calculated volume of the freshly prepared Dye Labeling Agent solution were added to the protein solution. Quickly, vortex to mix then briefly centrifuged to collect sample in the bottom of the tube. Wrapped the tube with aluminum foil to protect from light. Following incubation at room temperature for 60 min, unconjugated dye were removed by centrifuging the SpinOUT™ columns at 1,000 g for 6 min to collect the FITC-labeled r*Sm*CTSZ protein solution. FITC-labeled r*Sm*CTSZ (25 μl) were mixed with 10 μl bacteria and incubated at room temperature for 60 min, then applied in a 20 μl drop to the slide and allowed to settle for 30 min at room temperature, followed by viewing under fluorescence microscope. Negative control was similarly disposed, but just mixed FITC dye (25 μl) and 10 μl bacteria.

3. Results

3.1. Identification of turbot CTSZ gene

After searching the turbot databases using available CTSZ protein sequences from other species as queries, one cDNA and putative amino acid sequence of *Sm*CTSZ (GenBank accession: KY593343) were identified. In detail, the complete cDNA sequence of *Sm*CTSZ was 2069 bp in length, including a 5′ untranslated regions (UTR) of 201 bp, an open reading frame (ORF) of 954 bp and a 3′ UTR of 914 bp (Fig. 1). *Sm*CTSZ ORF encoded a 317 aa polypeptide with a predicted molecular mass of approximately 34.81 kDa and a theoretical pI of 6.36, with 6 protein kinase C phosphorylation sites, 2 casein kinase II phosphorylation sites, and 2 *N*-glycosylation sites (Table 2). Similar to other CTSZ protein, *Sm*CTSZ contains four active site triad residues (Gln^{92}, Cys^{101}, His^{250}, and Asn^{271}), which found in proteases of the papain family. There is also a unique insertion for CTSZ, which was embedded in a highly conserved peptide sequence CGSCW. For histidine residue, His^{250}, many studies have proven that it could adjacent to small amino acid residues, for example, glycine or alanine, followed by four aliphatic hydrophobic (Fig. 1). Four catalytic residues (Gln^{92}, Cys^{101}, His^{250}, and Asn^{271}) were found in a Pept C1 domain which was a highly conserved structure in the amino acid sequence of *Sm*CTSZ (Supplementary Fig. 1). In comparison to other species, turbot CTSZ showed the highest identity to killifish (*Fundulus heteroclitus*) with 80.4%, followed by *P. reticulata* (79.8%) and *L. crocea* (79.5%) (Table 3). Interestingly, turbot

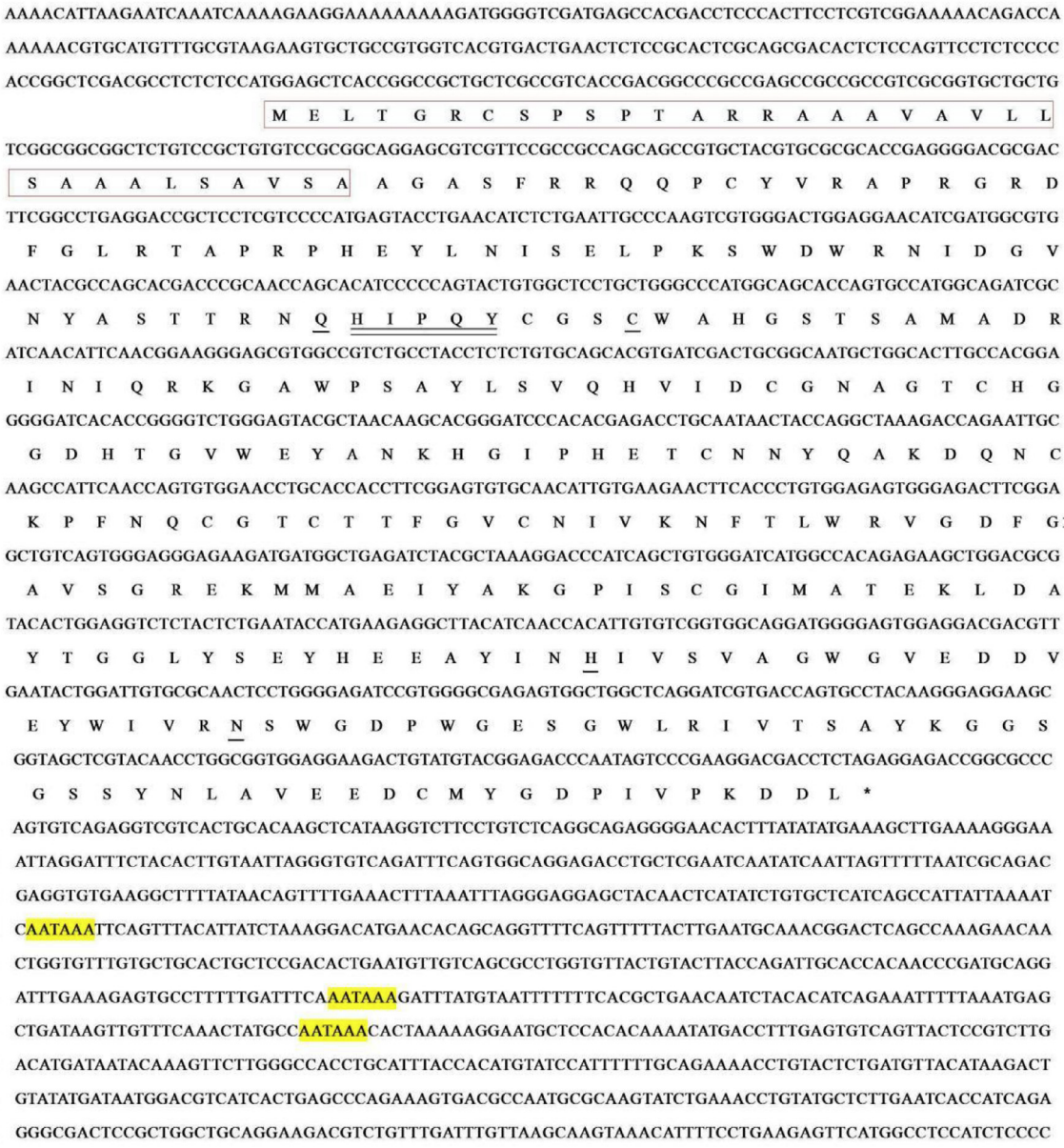

Fig. 1. The nucleotide and deduced amino acid sequences of *Sm*CTSZ. The putative signal peptide was boxed. The active site triad residues Gln[92], Cys[101], His[250], and Asn[271] are indicated in the thickly underlined. Mini loop HIPQY is double underline. The asterisk (*) at the end of the amino acid sequences shows the stop codon.

Table 2
Primary structural analysis. Properties of turbot CTSZ determined by ProtParam.

Protein	*Sm*CTSZ
No. of amino acids	317
Molecular weight	34808.93
Theoretical pI	6.36
Total No. of negatively charged residues (Asp + Glu)	32
Total No. of positively charged residues (Arg + Lys)	29
Formula	$C_{1526}H_{2310}N_{438}O_{463}S_{19}$
Instability index	42.84
Aliphatic index	65.30
Grand average of hydropathicity (GRAVY)	−0.397
Protein kinase C phosphorylation site	6
Casein kinase II phosphorylation site	2
N-glycosylation site	2

CTSZ showed the same similarity in *F. heteroclitus*, *P. reticulata*, and *L. crocea* for 87.4% (Table 3). In addition, prediction and analysis of secondary structure of CTSZ protein were employed the program of PRAI-GERLAND. The secondary structure of CTSZ protein was categorized in alpha helix (20.82%), random coil (62.46%) and extended strand (16.72%) (Supplementary Fig. 2). The secondary structure analyses of CTSZ showed that it has 12 b-sheets, 4 beta hairpins, 10 helix strands, 6 disulphide bonds, 22 beta turns, 2 γ-turns, 4 catalytic residues, and other structures (Fig. 2). Meanwhile, the tertiary structure of CTSZ was predicted by Phyre2. The 3D structure of CTSZ was 71% identical to d1deua with 100% confidence, and the image was colored by rainbow from N to C terminus (Fig. 3).

3.2. Phylogenetic and syntenic analysis of turbot gene

To further verify the gene identification, and determine the phylogenetic relationship of *Sm*CTSZ gene with other species, a neighbor-joining phylogenetic tree was constructed by MEGA7 (Fig. 4). Phylogenetic analysis of *Sm*CTSZ gene demonstrated the closest relationship

Table 3
Amino acid comparison of turbot CTSZ sequence with other species using MatGAT program. The upper triangle represents the amino acid identity, and the lower triangle represents the amino acid similarity.

	Turbot	*H.sapiens*	*M.musculus*	*G. gallus*	*C.picta*	*X.tropicalis*	*D.rerio*	*C.semilaevis*	*L.crocea*	*I.punctatus*	*E.lucius*	*P.reticulata*	*F.heteroclitus*
Turbot		65.6	65.3	71.9	70.0	70.1	72.0	77.6	79.5	69.5	76.1	79.8	80.4
H.sapiens	76.3		83.0	71.8	72.4	71.9	62.8	65.6	65.3	63.0	66.0	65.9	65.2
M.musculus	79.2	89.5		70.9	71.1	69.4	63.0	65.5	65.9	64.0	66.2	68.2	66.9
G. gallus	81.1	81.3	80.1		86.9	78.2	70.7	71.0	71.0	71.1	72.6	70.0	71.0
C.picta	80.4	80.3	79.7	91.8		79.0	70.0	70.2	71.8	71.8	72.5	71.5	72.2
X.tropicalis	77.9	81.5	78.1	86.9	88.2		70.8	72.1	74.3	71.3	75.4	75.3	74.7
D.rerio	82.0	76.2	76.5	82.3	82.2	81.1		76.4	79.9	81.7	83.1	78.6	78.1
C.semilaevis	85.5	79.3	80.1	81.0	81.9	80.3	86.2		83.2	75.4	78.8	81.3	81.3
L.crocea	87.4	80.2	79.1	83.9	84.2	83.5	86.8	91.4		78.7	82.9	87.1	86.5
I.punctatus	81.7	77.6	77.1	83.9	82.2	83.2	90.7	84.9	87.8		82.5	78.7	76.4
E.lucius	83.6	78.5	78.8	83.3	84.9	84.1	92.7	88.5	91.1	92.4		80.6	79.6
P.reticulata	87.4	79.2	80.7	83.6	83.2	84.2	88.1	89.1	92.4	88.1	90.4		91.1
F.heteroclitus	87.4	79.2	80.4	83.6	83.2	83.8	87.8	89.5	92.7	88.8	88.4	96.4	

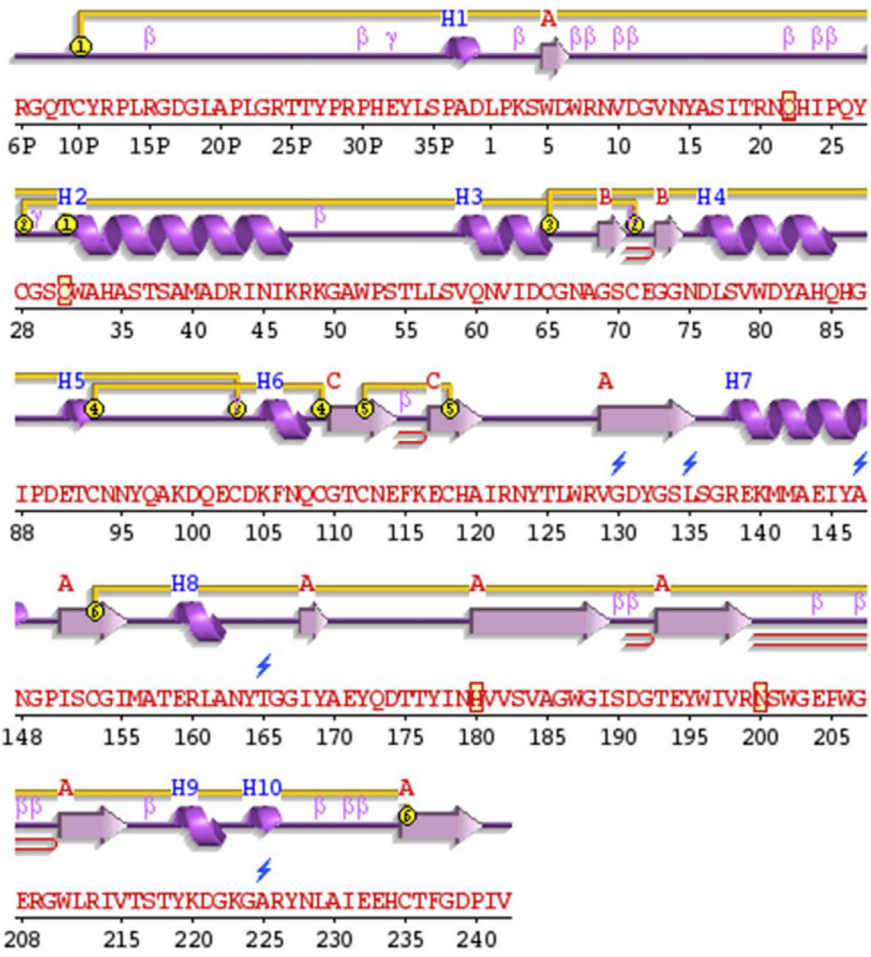

Fig. 2. Secondary structure of turbot CTSZ was predicted using PDBsum Generate. Sec. struc: (Helix Strand); Helices labeled: H1, H2, … and strands by their sheets A, B, …; β:beta turn; γ: gamma turn; beta hairpin; disulphide bond; catalytic residue; variant residue.

to the half smooth togue sole. All known fish CTSZ proteins, branched independently from the CTSZ protein of higher vertebrates (Fig. 4).

In order to strengthen phylogenetic analysis, syntenic analysis was carried out as an additional evidence for orthologies of the CTSZ gene. As shown in Fig. 5, the similar neighboring genes with CTSZ were identified in turbot as well as in fugu. In detail, the genomic neighborhood in turbot included Syntaxin 16 (stx16), Probable aminopeptidase NPEPL1 (pep11), which were presented in all this five species (Fig. 5), indicating a high conservation of CTSZ during evolution.

3.3. Analysis of CTSZ expression in normal turbot tissue

Quantitative expression analysis of *Sm*CTSZ in tissues of normal fish indicated that the highest expression level of CTSZ was in intestine, followed by head kidney, skin, and spleen (Fig. 6). Lower expression levels were observed in gill, liver and blood, and the lowest CTSZ expression level was detected in brain (Fig. 6).

3.4. Expression profiles of CTSZ gene following bacterial challenge

Following experimental challenge with *S. iniae*, the only down-regulation was observed in skin at 4 h with −2.78 fold, but it was

Fig. 3. The 3D structure of turbot CTSZ predicted using Phyre2. The tertiary structure of CTSZ was 86% identical to d1deua with 100% confidence, and the image was colored by rainbow from N to C terminus. Model dimensions (Å): X:50.418 Y:58.928 Z:49.345; 86% of residues were modelled at > 90% confidence.

quickly up-regulated with 22.84 fold at 8 h, and 49.20 fold at 12 h (Fig. 7). Of note, *Sm*CTSZ was up-regulated at all the timepoints following challenge in intestine and gill. The most up-regulation was observed in intestine with 73.42 fold at 4 h, as well as with 11.21 fold at 2 h, 38.35 fold at 8 h, and 26.54 fold at 12 h (Fig. 7). In gill, it was up-regulated with 6.63 fold at 2 h, 23.78 fold at 4 h, 19.47 fold at 8 h, and 23.79 fold at 12 h (Fig. 7).

In the *V. anguillarum* infection, *Sm*CTSZ was up-regulated at all the timepoints in all the examined tissues (Fig. 8). Similar to *S. iniae* challenge, the most up-regulation was also observed in intestine at 6 h with 57.72 fold, as well as with 43.63 fold at 2 h, 17.31 fold at 12 h, and 24.36 fold at 24 h (Fig. 8). In skin, the peak value was detected at 2 h with 37.80 fold, and then with 6.22 fold at 6 h, 29.75 fold at 12 h, and 13.41 fold at 24 h. In comparison to intestine and skin, the most up-regulation in gill was at 2 h with 4.55 fold, and then almost returned to basal levels at other timepoints (Fig. 8).

3.5. Microbial ligand binding in vitro

After IPTG induction, the recombinant protein r*Sm*CTSZ was purified, and a distinct band of r*Sm*CTSZ was revealed with a molecular weight of approximately 33 kDa by the method of SDS-PAGE (Fig. 9). From the WB profiles, antisera showed clear reaction with r*Sm*CTSZ and recognized r*Sm*CTSZ with molecular weights of about 33 kDa. An *in vitro* assay was employed to examine the binding ability of r*Sm*CTSZ with three microbial ligands (LPS, LTA and PGN). As shown in Fig. 10, an increased absorbance was observed with the increase of r*Sm*CTSZ concentrations in a solid-phase enzyme-linked immunosorbent assay (ELISA). In addition, the obvious affinity differences of r*Sm*CTSZ with microbial ligands were also observed, among which, the r*Sm*CTSZ showed the highest affinity with LPS, followed by PGN and LTA (Fig. 10).

3.6. Coagulant bacteria of FITC-labeled rSmCTSZ

To inspect the capacity of coagulant bacteria in r*Sm*CTSZ, green fluorescence were detected by FITC-labeled r*Sm*CTSZ coagulated with gram-negative bacteria (*V. anguillarum*, *E. coli*) and gram-positive bacteria (*S. agalactiae, S. iniae*). In bright field, some of bacteria were gathered, others were separated (Fig. 11 A1-D1). Most gathered bacteria showed strong green fluorescence (Fig. 11 A-D). FITC-labeled r*Sm*CTSZ had an effect on coagulating bacteria in these four bacteria.

4. Discussion

Cathepin Z (CTSZ) plays critical roles in protein turnover, cell type, the activity of macrophages, and innate immune regulation [6,30]. In the present study, the deduced polypeptide of *Sm*CTSZ consisted of 317 amino acids, and molecular weight of 34.80 kDa, which was similar to vertebrate and invertebrate (Table 2). The amino acid sequence of *Sm*CTSZ shared over 60% similarities with other identified CTSZs (Table 3). Moreover, structural analysis showed that *Sm*CTSZ possesses the typical structural characteristics of CTSZ, including a peptidase-C1 papain family cysteine protease domain (residues 80-303), a mini-loop (^{93}HIPQY^{97}) which is a unique feature of cathepsin Z/X members [31], and active site residues (Gln^{92}, Cys^{101}, His^{250}, and Asn^{271}) (Fig. 1). The cysteine residue Cys^{101} is embedded in a highly conserved peptide sequence, CGSCWA. The histidine residue His^{250} was adjacent to small amino acid residues, such as glycine or alanine, followed by four aliphatic hydrophobic residues (valine, leucine, isoleucine, and glycine) [14]. Asparagine was a component of the Asn-Ser-Trp (NSW) motif. These structural features of cysteine proteinases have also been

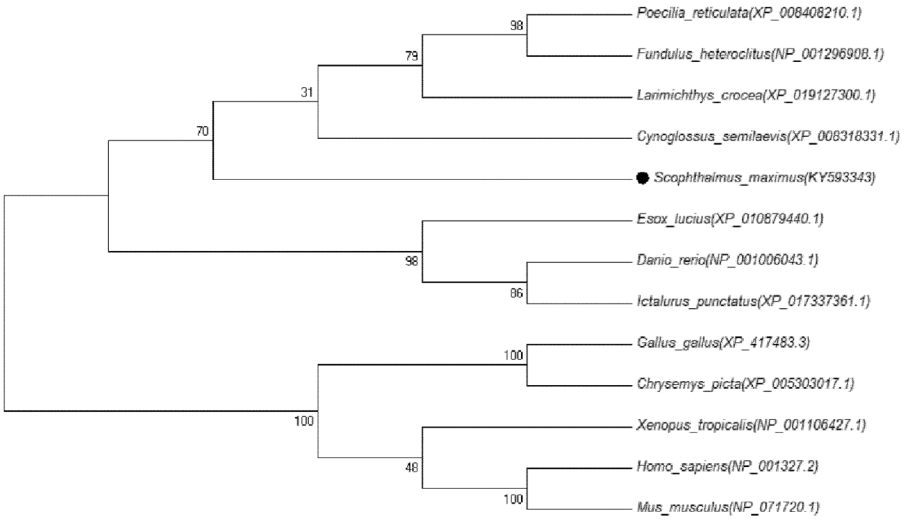

Fig. 4. Phylogenetic tree for the turbot CTSZ gene. The phylogenetic tree was constructed based on the amino acid sequences of CTSZ from species of fish and mammals, using the neighbor-joining method in MEGA 7. Gaps were removed by complete deletion and the phylogenetic tree was evaluated with 1000 bootstrap replications. The bootstrapping values were indicated by numbers at the nodes. Dark solid circles indicated the newly characterized turbot CTSZ gene.

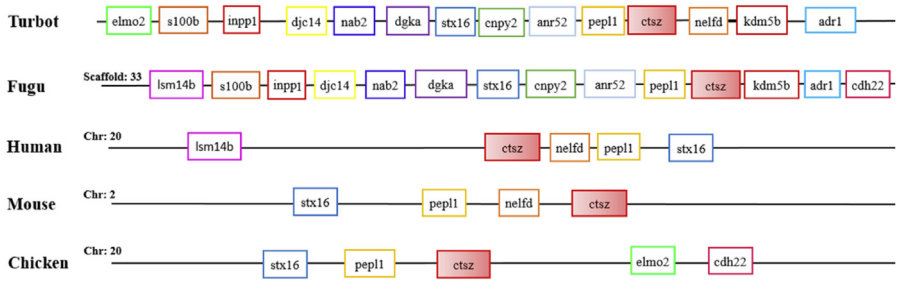

Fig. 5. Syntenic analysis of CTSZ gene from turbot, fugu, human, mouse and chicken. The CTSZ gene is highlighted by pinkish color filled boxes. elmo2: Engulfment and cell motility protein 2; s100b: Protein S100-B; inpp1: Inositol polyphosphate 1-phosphatase; djc14: DnaJ homolog subfamily C member 14; nab2: NGFI-A-binding protein 2; dgka: Diacylglycerol kinase alpha; stx16: Syntaxin 16; cnpy2: Protein canopy homolog 2; pepl1: Probable aminopeptidase NPEPL1; ctsz: capsin Z; nelfd: Negative elongation factor D; kdm5b: Lysine-specific demethylase 5B; adr1: Activated disease resistance protein 1; lsm14b: Protein LSM14 homolog B. (For interpretation of the references to color in this figure legend, the reader is referred to the Web version of this article.)

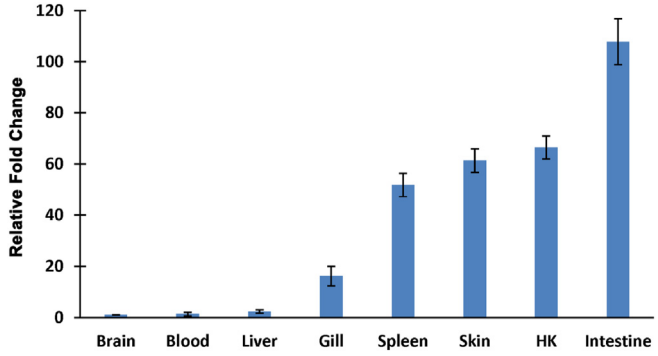

Fig. 6. Gene expression analysis of the CTSZ in different healthy turbot tissues. The expression level of CTSZ in brain was set as 1. HK was the abbreviation for head kidney.

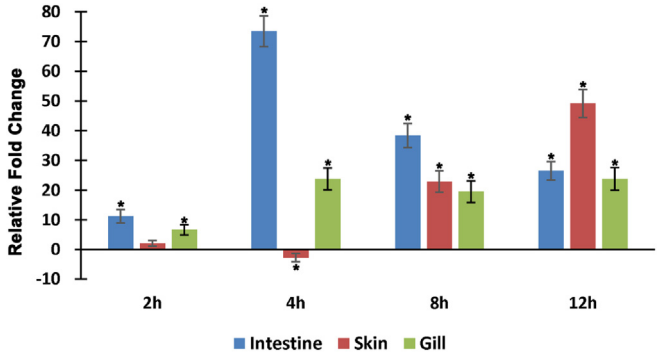

Fig. 7. Real-time qPCR analysis for *Sm*CTSZ expression following *Streptococcus iniae* infection. The *Sm*CTSZ expression levels were measured in the mucosal tissues including skin, gill, and intestine, at the time points of 2 h, 4 h, 8 h and 12 h post-infection. Fold change was calculated by the change in expression at a given time point relative to the untreated control and normalized by changes in the 18S housekeeping gene. The results were presented as mean ± SE of fold changes and the * indicated statistical significance at $P < 0.05$. Error bars indicated standard error (n = 3).

observed in *Sm*CTSZ (Fig. 1). A sequence alignment revealed that the CTSZ amino acid sequences were highly conserved and that the amino acid sequence of *Sm*CTSZ shared high overall sequence identity with teleost CTSZ homologs (Supplementary Fig. 1). A phylogenetic analysis indicated that *Sm*CTSZ was clustered with the CTSZ from half smooth togue sole (Fig. 4). The high sequence identity, together with the phylogenetic analysis and the structural features, indicated that *Sm*CTSZ is a new member of the vertebrate CTSZ subfamily.

To investigate the potential function of *Sm*CTSZ in turbot, the tissue distribution pattern was detected by qRT-PCR. In general, CTSZ was ubiquitously distributed in all the examined tissues, with higher expression levels in spleen, intestine and liver. In human, CTSZ was widely expressed in most tissues and cell lines [6]. In fish species, however, the tissue distribution of CTSZ was rarely studied, and just in

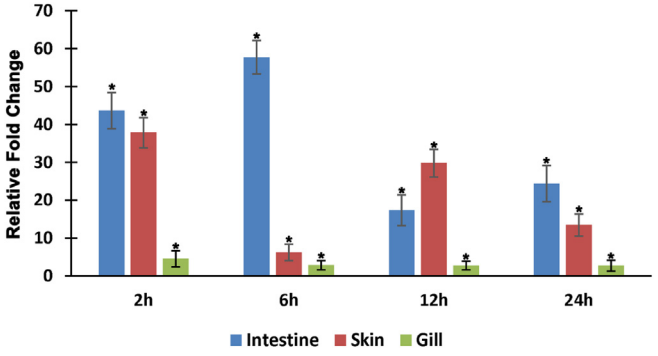

Fig. 8. Real-time qPCR analysis for *Sm*CTSZ expression levels following *Vibrio anguillarum* infection. The *Sm*CTSZ expression was measured in the mucosal tissues including skin, gill, and intestine at the time points of 2 h, 6 h, 12 h, and 24 h post-infection. Fold change was calculated by the change in expression at a given time point relative to the untreated control and normalized by change in the 18S housekeeping gene. The results were presented as mean ± SE of fold changes and * indicated statistical significance at $P < 0.05$. Error bars indicated standard error (n = 3).

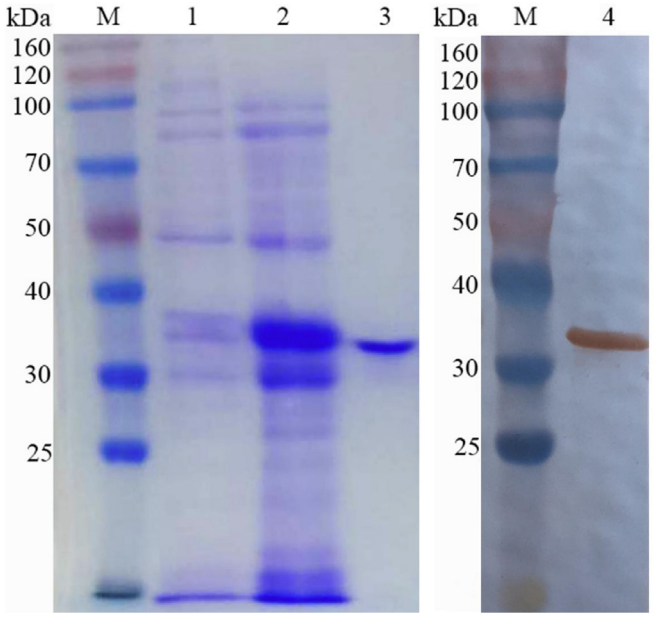

Fig. 9. SDS-PAGE analysis of r*Sm*CTSZ. Purified r*Sm*CTSZ (lane 4) was analyzed by SDS-PAGE and viewed after staining with Coomassie brilliant blue R-250. (For interpretation of the references to color in this figure legend, the reader is referred to the Web version of this article.)

two species, i.e., carp, olive flounder. However, in our study, the expression level of CTSZ in liver was not as high as carp and olive flounder, but was similarly highly expressed in intestine, head kidney,

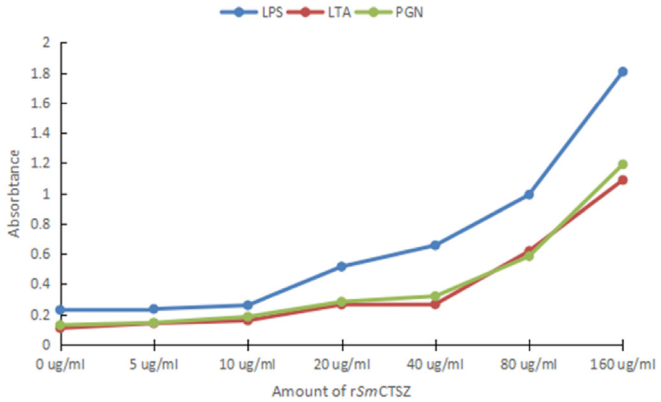

Fig. 10. Results of the *in vitro* binding assay of *Sm*CTSZ on microbial ligands, including lipopolysaccharide, peptidoglycan, and lipoteichoic acid.

skin and spleen. The different expression patterns across different species suggested CTSZ might play different roles in different species. Further studies are necessary to clear somewhat correlated, comparable results of CTSZ tissue distribution patterns in turbot and other organisms.

In order to elucidate the immune roles of *Sm*CTSZ in mucosal barriers, the expression profiles of CTSZ was characterized in turbot mucosal tissues (gill, skin and intestine) following bacterial infections, which are the first line of defence against pathogenic organisms. Here, one Gram-negative and one Gram-positive bacteria were selected to characterize and compare the expression signatures of CTSZ during infections. In general, following *V. anguillarum* and *S. iniae* infections, *Sm*CTSZ was significantly up-regulated in most tested tissues at most time points.

Post stimulation of *S. iniae*, *Sm*CTSZ was observed to be constitutively expressed in all the tested tissues, including gill, skin and intestine. Of note, *Sm*CTSZ was significantly up-regulated in all the timepoints in intestine and gill, and the highest expression level of *Sm*CTSZ was observed in intestine, which was much higher than other tissues. Cathepsins are a group of peptidases that involve in different levels of immune responses, including apoptosis, inflammation, and antigen processing [10]. Among different groups of cathepsins, CTSZ is ubiquitously expressed in most immune tissues, especially in immune cells [9]. Whereas there are plenty of immune cells (such as macrophages and monocytes) in intestine in teleost species, it might be hypothesized that *Sm*CTSZ could involve in the intestinal immune system of turbot. In disk abalone *Haliotis discus*, after *V. parahaemolyticus* and *Listeria monocytogenesthe* challenge, CTSZ was highly expressed in gill and hemocyte, which also indicated that CTSZ involved in host innate immune responses [32].

In case of *V. anguillarum* infection, *Sm*CTSZ gene was fast and significantly expressed in intestine at 2 h and reached the highest expression level at 6 h. While *Sm*CTSZ gene was significantly expressed at 2 h in skin, it almost declined to basal level at 6 h. The previous studies have suggested that intestine might serve as the primary portal of entry for *V. anguillarum* [33–35]. In rainbow trout (*Oncorhynchus mykiss*), intestine mucus has more mucus-associated components consisting of amino acids, carbohydrates and bile acids as chemoattractants for *V. anguillarum* than other mucus tissues [36]. In turbot, an oral challenge with *V. anguillarum* for turbot larvae could induce significant mortality, and 80% or more of the *V. anguillarum* cells were still attached to the turbot intestine after serial washings, indicating the strong adhesion and penetration abilities of *V. anguillarum* for turbot intestine [37]. Following administration of *V. anguillarum* by anal or intragastric intubation, the bacteria could be detected in turbot spleen as early as 2 h, indicating the ability of quickly pass through the intestine mucosal barrier [38]. In zebrafish following immersion infection, the intestine was the first site where the pathogen was detected [39]. Here, *Sm*CTSZ gene was also significantly up-regulated in skin following *V. anguillarum* challenge, indicating that the immune events happened extensively in skin to fight against the invasive *V. anguillarum*. It was highly possible that in the current study, skin was another main entry for *V. anguillarum* invasion, but the exact functions of CTSZ in turbot skin need to be verified in further studies.

To further understand the immunological roles of *Sm*CTSZ, the binding ability to different microbial ligands of its recombinant protein was determined *in vitro*. In our results, r*Sm*CTSZ exerted strong effect with lipopolysaccharide which is an outer membrane of Gram-negative bacteria, and it also showed strong binding ability with other tested microbial ligands, indicating the significant binding and transporting roles of *Sm*CTSZ. In addition, r*Sm*CTSZ have the highest binding ability with LPS, and the binding ability of PGN was a little higher than that of LTA, suggesting that *Sm*CTSZ might involved in the sensing and phagocytosis of bacterial pathogens, especially Gram-negative bacteria. Further studies are needed to explore more roles and functions of *CTSZ*

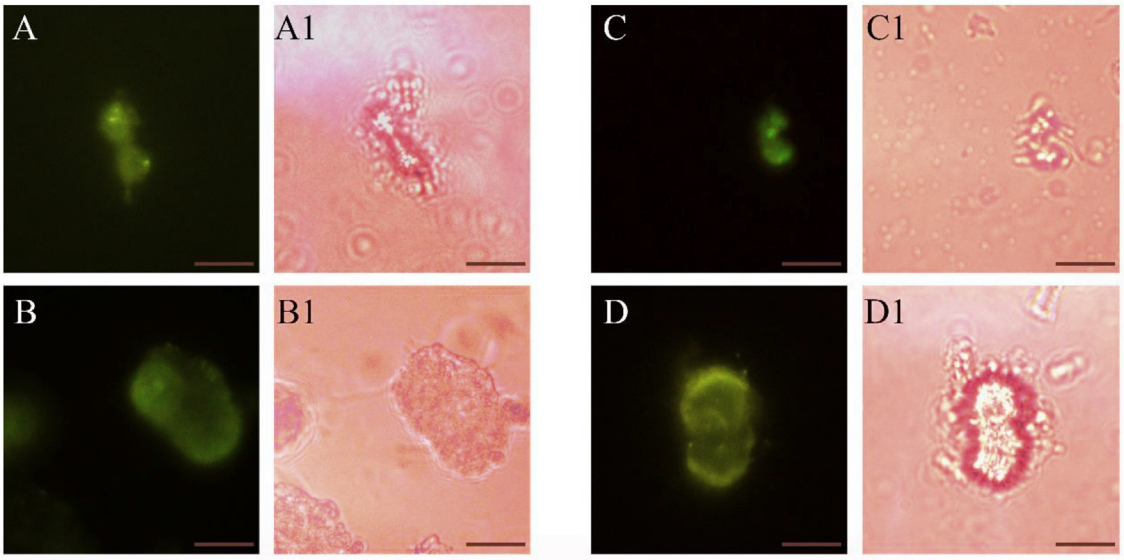

Fig. 11. Coagulant four species of bacteria of FITC-labeled r*Sm*CTSZ. A: *S. agalactiae*, B: *V. anguillarum*, C: *E. coli*, D: *S. iniae* were analyzed by fluorescence microscopy using FITC-labeled recombinant *Sm*CTSZ. A-D were FITC passage; A1-D1 were Bright Field. Scale bars represented 10 μm.

in order to elucidate the mechanism in turbot mucosal immunity.

So far, CTSZ gene have been identified in different species. Over the past few years, CTSZ has been identified in many mammal species to gain an understanding of potential roles in innate immunity against pathogen invasion. In human, LA Adams et al. found CTSZ was involved in susceptibility to tuberculosis [30]. And CTSZ could influence the macrophage migration, indicating a well-coordinated and distinct action of CTSZ in the inflammatory process after *Helicobacter pylori* infection [40]. CTSZ was also found to be involved in molting in *Caenorhabditis elegans* and in *Onchocerca vovulus* [41,42], in intracellular protein catabolism for enzyme in olive flounder [14], and in yolk metabolism in carp [12]. In addition, in killifish (*Fundulus heteroclitus*) and Salmon, CTSZ expression was relatively stable during oocyte growth and maturation [13,43], and CTSZ has been implicated in egg quality in rainbow [44]. Taken together, *Sm*CTSZ plays vital roles in different biological processes to contribute to mucosal homeostasis and barrier maintenance. However, the knowledge of CTSZ are still limited in teleost species, further studies should be carried out to better characterize its detailed roles in teleost mucosal immunity.

Acknowledgement

This study was supported by the National Science Foundation of China (No.:31602193). And it was also supported by keypoint research and invention program in Shandong Province (2017GHY215004).

Appendix A. Supplementary data

Supplementary data to this article can be found online at https://doi.org/10.1016/j.fsi.2018.10.046.

References

[1] H. Kirschke, B. Wiederanders, Lysosomal proteinases, Acta Histochem. 82 (1) (1987) 2–4.
[2] D. Nagler, R. Menard, Human cathepsin X: a novel cysteine protease of the papain family with a very short proregion and unique insertions, FEBS Lett. 434 (1–2) (1998) 135.
[3] K. Sol-Church, J. Frenck, D. Troeber, R.W. Mason, Cathepsin P, a novel protease in mouse placenta, Biochem. J. 343 Pt 2 (2) (1999) 307.
[4] E. Sakamoto, Y. Sakao, Y. Taniguchi, K. Yamafuji, Cathepsin Y (a novel thiol enzyme) produces kinin potentiating peptide from the component protein of rat plasma, Immunopharmacology 45 (1–3) (1999) 207.
[5] V. Dubljevic, J.W. Goding, A. Sali, A Conserved RGD (Arg-Gly-Asp) Motif in the Transferrin Receptor is Required for Binding to Transferrin vol. 341, (1999), pp. 11–14 (Pt 1)(1).
[6] I. Santamaría, G. Velasco, A.M. Pendás, A. Fueyo, C. López-Otín, Cathepsin Z, a novel human cysteine proteinase with a short propeptide domain and a unique chromosomal location, J. Biol. Chem. 273 (27) (1998) 16816–16823.
[7] G. Gunčar, I. Klemenčič, B. Turk, V. Turk, A. Karaoglanovic-Carmona, L. Juliano, D. Turk, Crystal structure of cathepsin X: a flip–flop of the ring of His23 allows carboxy-monopeptidase and carboxy-dipeptidase activity of the protease, Structure 8 (3) (2000) 305.
[8] R. Ménard, C. Therrien, P. Lachance, T. Sulea, H. Qo, A.D. Alvarezhernandez, W.R. Roush, Cathepsins X and B display distinct activity profiles that can be exploited for inhibitor design, Biol. Chem. 382 (5) (2001) 839–845.
[9] J. Kos, A. Sekirnik, A. Premzl, V.Z. Bergant, T. Langerholc, U. Repnik, B. Turk, B. Werle, R. Golouh, M. Jeras, Carboxypeptidases cathepsins X and B display distinct protein profile in human cells and tissues, Exp. Cell Res. 306 (1) (2005) 103–113.
[10] T. Zavasnikbergant, B. Turk, Cysteine cathepsins in the immune response, Tissue Antigens 67 (5) (2006) 349–355.
[11] J. Garin, M. Desjardins, The phagosome proteome: insight into phagosome functions, JCB (J. Cell Biol.) 152 (1) (2001) 165–180.
[12] C.M. Kao, F.L. Huang, Cloning and expression of carp cathepsin Z: possible involvement in yolk metabolism, Comp. Biochem. Physiol., B 149 (4) (2008) 541–551.
[13] M. Fabra, J. Cerdà, Ovarian cysteine proteinases in the teleost Fundulus heteroclitus: molecular cloning and gene expression during vitellogenesis and oocyte maturation, Mol. Reprod. Dev. 67 (3) (2004) 282–294.
[14] J.A. Sang, Y.K. Na, S.J. Jeon, H.S. Ji, E.J. Ju, J.S. Seo, M.S. Kim, J.K. Kim, J.K. Chung, H.H. Lee, Molecular cloning, tissue distribution and enzymatic characterization of cathepsin X from olive flounder (Paralichthys olivaceus), Comp. Biochem. Physiol., B 151 (2) (2008) 203–212.
[15] K. Tamura, G. Stecher, D. Peterson, A. Filipski, S. Kumar, MEGA6: molecular evolutionary Genetics analysis version 6.0, Mol. Biol. Evol. (2013) 2725–2729.
[16] L. Zhang, C. Gao, F. Liu, L. Song, B. Su, C. Li, Characterization and expression analysis of a peptidoglycan recognition protein gene, SmPGRP2 in mucosal tissues of turbot (Scophthalmus maximus L.) following bacterial challenge, Fish Shellfish Immunol. 56 (2016) 367–373.
[17] X. Dong, B. Su, S. Zhou, M. Shang, H. Yan, F. Liu, C. Gao, F. Tan, C. Li, Identification and expression analysis of toll-like receptor genes (TLR8 and TLR9) in mucosal tissues of turbot (Scophthalmus maximus L.) following bacterial challenge, Fish Shellfish Immunol. 58 (2016) 309–317.
[18] X. Dong, Q. Fu, S. Liu, C. Gao, B. Su, F. Tan, C. Li, The expression signatures of neuronal nitric oxide synthase (NOS1) in turbot (Scophthalmus maximus L.) mucosal surfaces against bacterial challenge, Fish Shellfish Immunol. 59 (2016) 406–413.
[19] C. Gao, Q. Fu, S. Zhou, L. Song, Y. Ren, X. Dong, B. Su, C. Li, The mucosal expression signatures of g-type lysozyme in turbot (Scophthalmus maximus) following bacterial challenge, Fish Shellfish Immunol. 54 (2016) 612–619.
[20] F. Liu, B. Su, C. Gao, S. Zhou, L. Song, F. Tan, X. Dong, Y. Ren, C. Li, Identification and expression analysis of TLR2 in mucosal tissues of turbot (Scophthalmus maximus L.) following bacterial challenge, Fish Shellfish Immunol. 55 (2016) 654–661.
[21] S.P. Biswas, A.G. Jadhao, R.C. Bhoyar, N.V. Palande, D.P. Sinh, Neuroanatomical localization of nitric oxide synthase (nNOS) in the central nervous system of carp, Labeo rohita during post-embryonic development, Int. J. Dev. Neurosci. 46 (2015) 14–26.
[22] C. Gao, Q. Fu, B. Su, S. Zhou, F. Liu, L. Song, M. Zhang, Y. Ren, X. Dong, F. Tan, Transcriptomic profiling revealed the signatures of intestinal barrier alteration and pathogen entry in turbot (Scophthalmus maximus) following Vibrio anguillarum challenge, Dev. Comp. Immunol. 65 (2016) 159–168.
[23] A. Figueras, D. Robledo, A. Corvelo, M. Hermida, P. Pereiro, J.A. Rubiolo, J. Gómezgarrido, L. Carreté, X. Bello, M. Gut, Whole genome sequencing of turbot (Scophthalmus maximus; Pleuronectiformes): a fish adapted to demersal life, DNA Res. 23 (2016) 181–192 3(2016-3-6) 23(3).
[24] E. Gasteiger, C. Hoogland, A. Gattiker, S.E. Duvaud, M.R. Wilkins, R.D. Appel, A. Bairoch, Protein identification and analysis tools on the ExPASy server, Methods Mol. Biol. 112 (112) (1999) 531.
[25] S. John, B. Ledion, J.J. Campanella, MatGAT, An application that generates similarity/identity matrices using protein or DNA sequences, BMC Bioinf. 4 (1) (2003) 29.
[26] F. Sievers, A. Wilm, D. Dineen, T.J. Gibson, K. Karplus, W. Li, R. Lopez, H. Mcwilliam, M. Remmert, J.D. Thompson, Fast, scalable generation of high uality protein multiple sequence alignments using Clustal Omega, Mol. Syst. Biol. 7 (1) (2011) 539.
[27] S. Kumar, G. Stecher, K. Tamura, MEGA7: molecular evolutionary Genetics analysis version 7.0 for bigger datasets, Mol. Biol. Evol. 33 (7) (2016) 1870.
[28] M. Muffato, A. Louis, C.E. Poisnel, H.R. Crollius, Genomicus, Bioinformatics 26 (8) (2010).
[29] M.W. Pfaffl, G.W. Horgan, L. Dempfle, Relative expression software tool (REST©) for group-wise comparison and statistical analysis of relative expression results in real-time PCR, Nucleic Acids Res. 30 (9) (2002) e36.
[30] L.A. Adams, M. Möller, A. Nebel, S. Schreiber, d.M.L. Van, P.D. van Helden, E.G. Hoal, Polymorphisms in MC3R promoter and CTSZ 3'UTR are associated with tuberculosis susceptibility, Eur. J. Human Genet. Ejhg 19 (6) (2011) 676.
[31] D.K. Nägler, R. Zhang, W. Tam, T. Sulea, E.O. Purisima, R. Ménard, Human cathepsin X: a cysteine protease with unique carboxypeptidase activity, Biochemistry 38 (39) (1999) 12648–12654.
[32] G.I. Godahewa, P. Ncn, S. Lee, M.J. Kim, J. Lee, A cysteine protease (cathepsin Z) from disk abalone, Haliotis discus discus: genomic characterization and transcriptional profiling during bacterial infections, Gene 627 (2017) 500–507.
[33] X. Cai, C. Gao, B. Su, F. Tan, N. Yang, G. Wang, Expression profiling and microbial ligand binding analysis of high-mobility group box-1 (HMGB1) in turbot (Scophthalmus maximus L.), Fish Shellfish Immunol. (2018) 100–108.
[34] L. Chao, C. Gao, F. Qiang, B. Su, J. Chen, Identification and expression analysis of fetuin B (FETUB) in turbot (Scophthalmus maximus L.) mucosal barriers following bacterial challenge, Fish Shellfish Immunol. 68 (2017).
[35] C. Gao, B. Su, D. Zhang, Y. Ning, S. Lin, F. Qiang, S. Zhou, F. Tan, L. Chao, l -rhamnose-binding lectins (RBLs) in turbot (Scophthalmus maximus L.): characterization and expression profiling in mucosal tissues, Fish Shellfish Immunol. 80 (2018) 264–273.
[36] R. O'Toole, S. Lundberg, S. Fredriksson, A. Jansson, N. Bo, H. Wolfwatz, The chemotactic response of Vibrio anguillarum to fish intestinal mucus is mediated by a combination of multiple mucus components, J. Bacteriol. 181 (14) (1999) 4308–4317.
[37] M. Chair, M. Dehasque, S.V. Poucke, H. Nelis, P.D. Sorgeloos, A.P.D. Leenheer, An oral challenge for turbot with Vibrio anguillarum, Aquacult. Int. 2 (4) (1994) 270–272.
[38] J.C. Oisson, A. Jöborn, A. Westerdahl, L. Blomberg, S. Kjelleberg, P.L. Conway, Is the turbot, Scophthalmus maximus (L.), intestine a portal of entry for the fish pathogen Vibrio anguillarum? J. Fish. Dis. 19 (3) (1996) 225–234.
[39] R. O'Toole, J.V. Hofsten, R. Rosqvist, P.E. Olsson, H. Wolf-Watz, Visualisation of Zebrafish infection by GFP-labelled Vibrio anguillarum, Microb. Pathog. 37 (1) (2004) 41–46.
[40] A. Bernhardt, D. Kuester, A. Roessner, T. Reinheckel, S. Krueger, Cathepsin X-deficient gastric epithelial cells in co-culture with macrophages: characterization of cytokine response and migration capability after Helicobacter pylori infection, J. Biol. Chem. 285 (44) (2010) 33691–33700.
[41] S. Hashmi, J. Zhang, Y. Oksov, S. Lustigman, The Caenorhabditis elegans cathepsin Z-like cysteine protease, Ce-CPZ-1, has a multifunctional role during the worms'

development, J. Biol. Chem. 279 (7) (2004) 6035–6045.
[42] S. Lustigman, J. Zhang, J. Liu, Y. Oksov, S. Hashmi, RNA interference targeting cathepsin L and Z-like cysteine proteases of Onchocerca volvulus confirmed their essential function during L3 molting, Mol. Biochem. Parasitol. 138 (2) (2004) 165–170.
[43] J.A. Luckenbach, D.B. Iliev, F.W. Goetz, P. Swanson, Identification of differentially expressed ovarian genes during primary and early secondary oocyte growth in coho salmon, Oncorhynchus kisutch, Reprod. Biol. Endocrinol. 6 (1) (2008) 1–15.
[44] J. Bobe, T. Nguyen, B. Jalabert, Targeted gene expression profiling in the rainbow trout (Oncorhynchus mykiss) ovary during maturational competence acquisition and oocyte maturation, Biol. Reprod. 71 (1) (2004) 73–82.